
GalaxiesML: a dataset of galaxy images, photometry, redshifts, and structural parameters for machine learning

Tuan Do

Physics and Astronomy Department
UCLA
Los Angeles, CA 90095
tdo@astro.ucla.edu

Bernie Boscoe

Computer Science Department
Southern Oregon University
Ashland, OR 97520
boscoeb@sou.edu

Evan Jones

Physics and Astronomy Department
UCLA
Los Angeles, CA 90095
ejones@astro.ucla.edu

Yun Qi Li

Physics and Astronomy Department
UCLA
Los Angeles, CA 90095
yunqil@g.ucla.edu

Kevin Alfaro

Physics and Astronomy Department
UCLA
Los Angeles, CA 90095
keal1885@gmail.com

Abstract

We present a dataset built for machine learning applications consisting of galaxy photometry, images, spectroscopic redshifts, and structural properties. This dataset comprises 286,401 galaxy images and photometry from the Hyper-Suprime-Cam Survey PDR2 in five imaging filters (g, r, i, z, y) with spectroscopically confirmed redshifts as ground truth. Such a dataset is important for machine learning applications because it is uniform, consistent, and has minimal outliers but still contains a realistic range of signal-to-noise ratios. We make this dataset public to help spur development of machine learning methods for the next generation of surveys such as Euclid and LSST. The aim of GalaxiesML is to provide a robust dataset that can be used not only for astrophysics but also for machine learning, where image properties cannot be validated by the human eye and are instead governed by physical laws. We describe the challenges associated with putting together a dataset from publicly available archives, including outlier rejection, duplication, establishing ground truths, and sample selection. This is one of the largest public machine learning-ready training sets of its kind with redshifts ranging from 0.01 to 4. The redshift distribution of this sample peaks at redshift of 1.5 and falls off rapidly beyond redshift 2.5. We also include an example application of this dataset

for redshift estimation, demonstrating that using images for redshift estimation produces more accurate results compared to using photometry alone. For example, the bias in redshift estimate is a factor of 10 lower when using images between redshift of 0.1 to 1.25 compared to photometry alone. Results from dataset such as this will help inform us on how to best make use of data from the next generation of galaxy surveys.

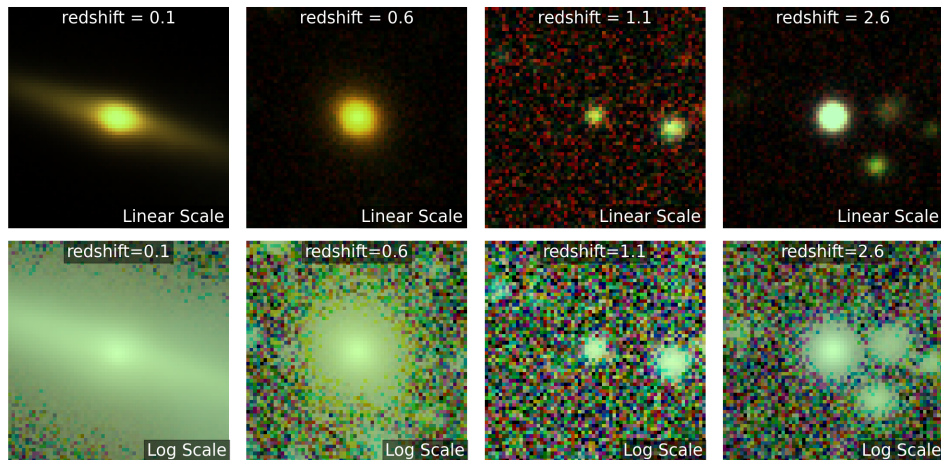


Figure 1: Example of galaxies at different redshifts from the GalaxiesML dataset. The top row shows the images in a linear intensity scale while the bottom row shows the images in a logarithmic scale to show lower surface brightness features like nearby galaxies .

1 Introduction

One of the major questions in physics and astrophysics is the nature of dark matter and dark energy. Together, dark matter and dark energy make up over 95% of the energy density of the universe, yet we do not know their particle or field nature [12]. The most promising approach to investigating their nature is through observations of the Universe on cosmic scales, pushing the limits of not only our telescopes and instrumentation, but also of our data analysis techniques.

Machine learning holds potential to help achieve the ambitious science goals of the large experiments in Astrophysics that are coming online now and in the next few years. The vast majority of data we have about the Universe is in the form of images, which are not always easily interpreted. For example, a key measurement required is how galaxies are spatially distributed across different cosmic times, but the distance to a galaxy (redshift) is not easily determined from its images alone. Fortunately, because the properties of galaxies evolve over time according to physical laws, the images of galaxies at different wavelengths encode information about how long ago their light was emitted, which in turn enables the determination of their distance. The relationship between the images of galaxies and their redshifts is complex due to the diversity of their formation pathways. Mapping this relationship is an ideal problem for machine learning [e.g., 32].

While astronomy has often led the way in the sciences for open access to data, there are not many datasets specifically designed for machine learning. Astronomical data is typically available through data archives as raw or processed data products for individual objects. Although these data products usually meet the needs of most researchers, machine learning applications require a higher level of data curation and compilation to ensure accurate predictions [7]. Creating valid, replicable datasets is often one of the most time-consuming facets of the machine learning process [40].

Large science surveys such as the Large Survey in Space and Time (LSST) [20] and the Euclid mission [11] aim to observe billions of galaxies to map their distribution throughout cosmic time, with the goal of constraining models of dark matter and dark energy. These surveys are expected to produce data at scales orders of magnitude larger than what we currently possess.

To efficiently analyze and leverage these vast datasets, astronomers have increasingly turned to machine learning methods. Machine learning models are particularly useful for problems where calculating likelihoods is challenging, especially when large datasets for training and sufficient computing resources are available. Extracting information from images falls into this category. For instance, accurately estimating redshifts from images is critical for achieving LSST’s cosmology goals. spectroscopy is too time-consuming and expensive to apply to the billions of galaxies required for measuring sensitive cosmological parameters [e.g., 28]. Because it is unclear how to analytically compute redshifts from vast numbers of images, machine learning offers a data-driven solution to this challenge. In astronomy, images are a primary source of information, but their resolutions vary as more distant objects are captured. As the data collection grows, the task of ground truthing continually evolves. Human judgment cannot be relied upon to assess images ‘by eye’ in traditional machine learning benchmarking methods; instead, other methods must be used to determine the accuracy of models’ predictions.

In this work, we present GalaxiesML, a new publicly available dataset of 286,401 galaxy images in five wavelength filters and galaxy properties specifically designed for machine learning applications. While the dataset has primarily been used for photometric redshift estimation, it is versatile and can support other science goals as well. It is based on publicly available survey data, including images, photometry, and spectroscopic redshifts. The spectroscopic redshifts serve as the ground truth for the redshifts associated with the images. Additional processing has been performed to measure the morphological information for each galaxy image. We chose to use the Hyper-Suprime-Cam (HSC) Survey [2] as the basis for this dataset because it provides a representative sample of galaxies comparable to those expected from the next generation of large sky surveys. GalaxiesML is optimized for machine learning models by carefully addressing issues like outliers and missing data, and the images and tabular data are provided in a format that can be easily integrated into modern machine learning frameworks.

By releasing this dataset, we aim to provide: (1) a large source of training data, (2) a consistent dataset for model comparisons, (3) a reduction in barriers to entry for applying machine learning in cosmology, and (4) a fixed dataset that enables reproducibility of findings. We also hope that this dataset will be valuable to general machine learning practitioners as an alternative to other imaging datasets, offering data from a scientific domain where the images are directly related to physical laws.

2 Related Work

Astronomers have been using machine learning for decades. Examples from the past decade include the morphological classification of galaxies using training data crowd-sourced from GalaxyZoo [26] which demonstrated that deep neural networks can perform as accurately as humans in classifying galaxies [16]. In exoplanet science, [36] showed that convolutional neural networks can effectively detect planets in light curves measured by the Kepler spacecraft. The AstroML project [21] has compiled both analysis tools and datasets that are useful for machine learning in astrophysics. However, these datasets are relatively small and are primarily intended for demonstrating how models work. They do not present significant challenges for new deep learning models nor do they represent the realistic test cases that will arise from the next generation of telescopes. Additionally, the datasets used in machine learning research papers in astronomy are often not published or are specifically designed to test a single algorithm [3, 5, 6, 9, 14, 17, 19, 31, 34, 35, 38, 39, 41]. Despite major advances in available quality data and sophisticated tooling, the growth of publicly available astronomy machine learning datasets has been slow. For example, there are no astronomy datasets available in the Tensorflow dataset repository or the University of California, Irvine (UCI) machine learning repository. While Kaggle hosts several toy astronomy datasets in various user repositories, none of them are comparable to GalaxiesML in terms of scale and scientific applicability.

3 The GalaxiesML Dataset

The primary data sources for this work are from the HSC Survey Data Release 2 and the associated spectroscopic redshift database[2]. This survey is conducted using the 8-meter diameter Subaru Telescope, located on Maunakea, a mountain in Hawaii. The HSC survey PDR2 is a sky survey over 300 square degrees of the sky and contains images of over 30 million galaxies in the g, r, i, z, y imaging filters. The HSC survey reaches a similar depth as upcoming large sky surveys, but over

smaller region of the sky, which makes this survey a good precursor to train and test machine learning models. The HSC PDR2 database contains spectroscopic redshifts cross-matched by the team (within a projected distance of $< 0.5''$) to the HSC catalog using of publicly available spectroscopic redshift catalogs [25, 8, 29, 37, 30, 24, 18, 27, 15, 33, 10, 13].

We assemble the dataset in 6 major stages:

1. Query and download from the HSC PDR2 and spectroscopic redshift databases
2. Apply additional data quality filters & remove duplicates and outliers
3. Download images and produce cutouts
4. Fit images to determine morphological information
5. Save the dataset into ML compatible formats

These stages are shown in the flow chart in Fig. 2 and outlined below.

3.1 Database Queries

We create a custom SQL query to select and download data from the HSC Survey PDR2 Archive [2]. The initial selection of galaxies is designed to include as many well-observed galaxies as possible. We use the following criteria for selecting galaxies from the PDR2 database:

- `grizy_cmodel_flux_flag = False` $z > 0$
- `grizy_pixelflags_edge = False`
- `grizy_pixelflags_interpolatedcenter = False`
- `grizy_pixelflags_saturatedcenter = False`, unique galaxy object ID
- `grizy_pixelflags_crcenter = False`,
- `grizy_pixelflags_bad = False`
- `grizy_sdsscentroid_flag = False`

For photometric redshift applications, the dataset needs a source of 'truth' for the redshift of each galaxy, so we also require that the objects have reliable spectroscopic redshift measurements by joining the tables with the spectroscopic redshift tables in the HSC database. We use the spectroscopic redshift information gathered by the HSC team as the ground truth for this sample. For detail of this process, see [2]. In brief, a match was made between the location of objects in the HSC survey with those from multiple spectroscopic surveys. We find that sample of objects from step X has Y counterparts with spectroscopic redshift information. In addition to joining with the photometry table, we also apply the following filters for the redshifts:

- $z > 0$
- $z \neq 9.9999$
- $0 < z_{err} < 1$
- `specz_flag_homogeneous = True`

We require that the galaxies be detected in all 5 imaging filters. The database query is reproduced in Appendix A. Overall, this initial sample has 801,246 objects.

3.2 Additional data quality filters & remove duplicates

We applying the following additional filters to the list of galaxies after extract the objects from the database:

- Redshift range: $0.01 < z < 4.0$
- Spectroscopic redshift error: $\sigma_{specz} < 0.005/(1 + specz)$
- Magnitude range in all bands: $0 < \{band\}_cmodel_mag < 50$

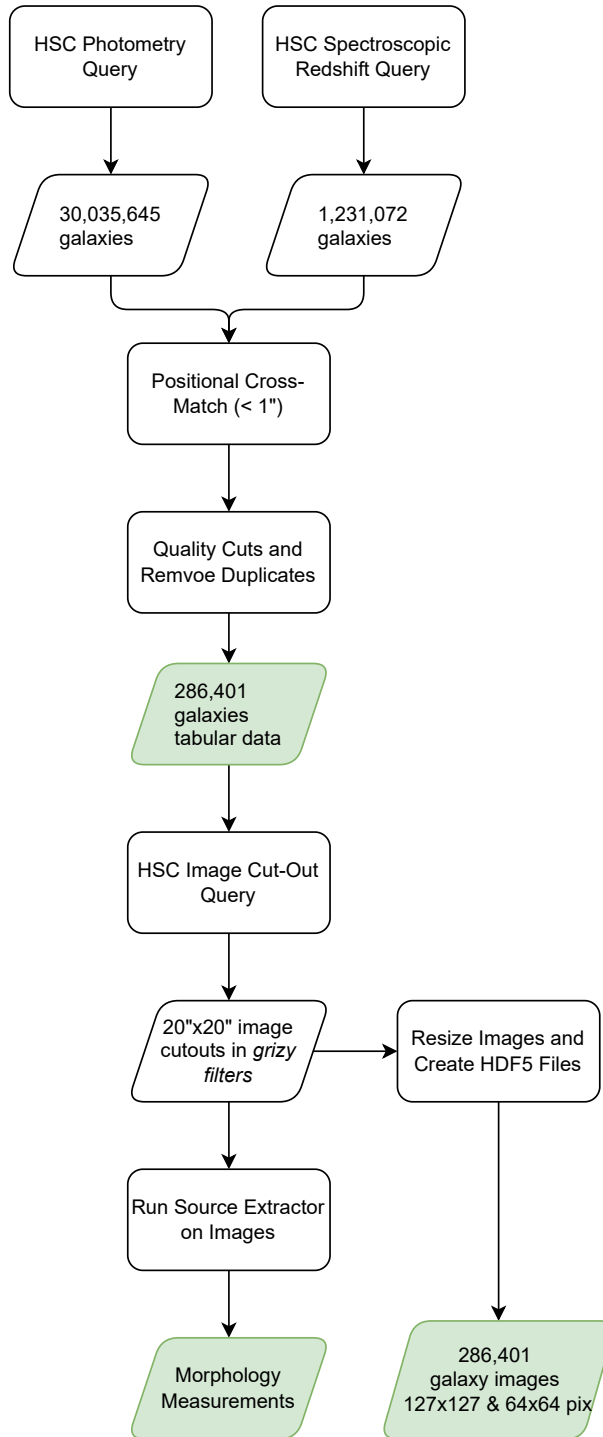


Figure 2: Flow chart showing the steps used in creating the GalaxiesML dataset. Rectangles represent processes and parallelograms are the products. The green parallelograms are the datasets that are part of the release.

To build our final sample, we then remove duplicate objects from the sample. While each row has a unique ObjID in the database, there can be multiple Object IDs for the same physical source because there were multiple measurements of its photometry. About 70% of the entries do not refer to unique

sources. We define duplicates as objects that have the same spectroscopic redshift identifier. Note that the spectroscopic redshifts were matched to the photometry using a distance of 0.5 arcseconds by the HSC team ¹. We also identify duplicate sources with the same HSC object ID, but different spectroscopic IDs. In the case of duplicates, we keep the first match and remove the others. After this stage, our final sample includes 286,401 sources.

3.3 Download and produce image cutouts

After obtaining the final sample of galaxies, we query the HSC PDR2 cutout service to download the images² (see Supplemental). We submit queries at the RA and DEC for each band in batches of 100,000 galaxies at a time, with cutout sizes of $10'' \times 10''$. We download the coadd option for images and selected the PDR2 Wide option. The images are downloaded as FITS files, with one in each band.

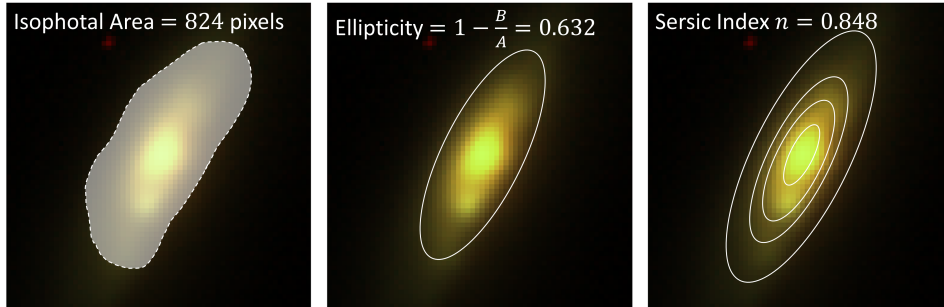


Figure 3: Example of the morphological parameters measured on a low redshift galaxy (Object ID 36416246018753893, $z = 0.0713$) using Source Extractor. **Left:** isophotal area, **center:** ellipticity, **right:** Sersic Index.

3.4 Measurement of the Morphological Parameters

We also extracted typical morphological features from the galaxy images to aid in interpreting the images and models. The 127×127 pixel images were fit using Source Extractor [4]. Source Extractor is a tool that is often used to model galaxies in images. Source Extractor fits the pixel values of images using parameterized models of galaxies using an estimate of the point spread function (PSF). It can fit for multiple sources at once and produce a segmentation map that indicates which pixels belong to which source. We parameterized the morphology of the galaxies using several models:

- Elliptical model - fitting the sources as an ellipse with a semi-major axis, semi-minor axis, and orientation.
- Sersic model - fit the flux distribution with a Sersic profile
- Isophotal, half-light, and Petrosian radius.

We also determine the number of galaxies in the image from the image segmentation map from Source Extractor. Source Extractor identifies sources using a detection threshold of pixel values above the background (called DETECT_THRESH), which we set to 3σ . We use the source position parameters X_IMAGE and Y_IMAGE closest to the center of the image as the galaxy that is associated with the spectroscopic redshift from the HSC catalog. We also utilize the position parameters to identify the number of other galaxies in a circle with a radius of 15, 10, and 5 pixels around the center of the image to quantify the number of nearby sources. The complete Source Extract configuration file we use for each galaxy is reproduced in Supplemental Materials.

¹https://hsc-release.mtk.nao.ac.jp/doc/index.php/dr1_specz/

²https://hsc-release.mtk.nao.ac.jp/das_cutout/pdr2/

Table 1: GalaxiesML Column Definition - Galaxy Properties & Morphology Measurements

Column Name	Units	Description
object_id		object ID from the HSC survey. Unique ID in 64bit integer
coord	(deg, deg, deg)	Coordinate used in coneSearch(coord, RA, DEC, RADIUS)
ra	deg	RA (J2000.0) of the image center
dec	deg	DEC (J2000.0) of the image center
{band}_cmodel_mag	mag	magnitude of the central galaxy in filter {band}
{band}_cmodel_magsigma	mag	uncertainty in the magnitude in filter {band}
skymap_id		location of the galaxy in internal survey position definition (t
specz_name		name(s) of the galaxy in the spectroscopic survey(s)
specz_flag_homogeneous		Homogenized spec-z flag. (TRUE=secure, FALSE=insecure)
specz_mag_i	mag	i-band magnitude of the galaxy in the spectroscopic survey
specz_ra	deg	RA (J2000.0) of galaxy in spectroscopic survey
specz_dec	deg	DEC (J2000.0) of galaxy in spectroscopic survey
specz_redshift		spectroscopic redshift
specz_redshift_err		spectroscopic redshift uncertainty
{band}_central_image_pol_15px_rad		See Section 4
{band}_central_image_pop_10px_rad		See Section 4
{band}_central_image_pop_5px_rad		See Section 4
{band}_ellipticity	pixels	See Section 4
{band}_half_light_radius	pixels	See Section 4
{band}_isophotal_area	pixels	See Section 4
{band}_major_axis	pixels	See Section 4
{band}_minor_axis	pixels	See Section 4
{band}_peak_surface_brightness	mag/sq. arcsec	See Section 4
{band}_petro_rad	pixels	See Section 4
{band}_pos_angle	deg	See Section 4
{band}_sersic_index		See Section 4
{band}_total_galaxies		See Section 4

3.5 Save the dataset into ML compatible format

The imaging data is stored in the HDF5 file format. This file contains cutouts of each galaxy image in g, r, i, z, y , stored in the `image` key of the HDF5 file as an $N_{gal} \times N_x \times N_y$ array. The decision to use HDF5 is due to its support for reading in only parts of the dataset at a time, and for its ease of use in machine learning frameworks. To create the HDF5, we download the images of each object in all five HSC imaging filters in the FITS format and combine the data into HDF5 files. The data are downloaded as cutouts from larger scale HSC images using the HSC cutout service³. We use an image radius query of `sh = 10arcseconds, sw = 10arcseconds`, which results in images of 20×20 arcseconds in spatial dimension. The images have a plate scale of 0.168 arcseconds per pixel [1]. We created two image sizes: 127x127 pix and 64x64 pix. Most machine learning methods require all images to have fixed sizes. Having multiple options for the image sizes allows one to test the effect of image sizes on model performance and to use wider variety of models. For each image size we create 3 HDF5 files for training (60%), validation (20%), and testing (20%) by randomly splitting the data. We perform the split for convenience and to more easily compare model performances with the same split.

4 Description of ML Dataset

The GalaxiesML dataset is a collection of tabular data, imaging data, and metadata. The tabular data is organized as a CSV file and also included in the HDF5 files with the images. In the HDF5, the images ($5 \times 127 \times 127$ or $5 \times 64 \times 64$) are under the `image` key, while the other tabular data are under the keys corresponding to their column name. The tabular data providing detailed information on the identification and characteristics of each galaxy sourced from the HSC and spectroscopic database. The tables also include the extracted features including morphology.

³https://hsc-release.mtk.nao.ac.jp/das_cutout/pdr2/

The following columns are the list of extracted parameters using Source Extractor:

- `{band}_central_image_pol_15px_rad`: The number of detected objects within a 15-pixel-radius circle, centered at the middle of the image. Derived from Source Extractor segmentation file.
- `{band}_central_image_pop_10px_rad`: The number of detected objects within a 10-pixel-radius circle, centered at the middle of the image. Derived from Source Extractor segmentation file.
- `{band}_central_image_pop_5px_rad`: The number of detected objects within a 5-pixel-radius circle, centered at the middle of the image. Derived from Source Extractor segmentation file.
- `{band}_ellipticity`: The ellipticity of the object, defined as $1 - B/A$. Where B is the semi-minor axis of an object and A is the semi-major axis (pixels).
- `{band}_half_light_radius`: The radius of an object at which 50% of the flux is contained (pixels).
- `{band}_isophotal_area`: The total number of pixels that a detected object is composed of.
- `{band}_major_axis`: Major axis of the detected object (pixels).
- `{band}_minor_axis`: Minor axis of the detected object (pixels).
- `{band}_peak_surface_brightness`: The peak surface brightness above background of the object (magnitudes per square arcsecond).
- `{band}_petro_rad`: Petrosian radius of an object (pixels).
- `{band}_pos_angle`: Rotation of the major axis with respect to the x-axis of the image plane, counterclockwise (degrees).
- `{band}_sersic_index`: The Sérsic index of the object, which describes the shape of the object's light profile.
- `{band}_total_galaxies`: Total number of galaxies detected by Source Extractor in an image.

The data is available from Zenodo with a DOI: [10.5281/zenodo.11117528](https://doi.org/10.5281/zenodo.11117528).

5 GalaxiesML Use: Neural Networks for Redshift Predictions

The publications using GalaxiesML include that of [23], which developed the first Bayesian neural networks for photometric redshifts (Fig. 4). This work found that Bayesian neural networks can provide accurate uncertainties for the redshift predictions, which is crucial for scientific use of the predictions in cosmology. In addition [22] found these networks were mostly robust to out-of-distribution biases and can provide good uncertainty estimates even for faint and low signal to noise galaxies.

6 Discussion and Conclusion

We have introduced GalaxiesML, a machine learning ready dataset designed for use by both astrophysicists or learners desiring to use a dataset with a scientific aim that includes noise and a ground truth derived from spectroscopic data rather than human visual assessment. GalaxiesML can be used in a variety of applications with or without the inclusion of image data. The dataset's size, $\sim 300,000$ galaxies and over 100 features allows for scientific exploration that is "medium sized" (116GB) that can be efficiently loaded into common machine learning tools, such as Jupyter notebooks, or run on GPU-enabled machines with a reasonable number of cores. It is designed to be within the reach of individual researchers while also being publicly accessible.

Our goal is to provide additional resources to make this dataset useful for scientific exploration, education, and benchmarking. We also aim to ensure compatibility with popular dataloader APIs, facilitating easier integration into machine learning workflows. GalaxiesML represents an important contribution to the growing collection of scientific datasets designed specifically for machine learning applications.

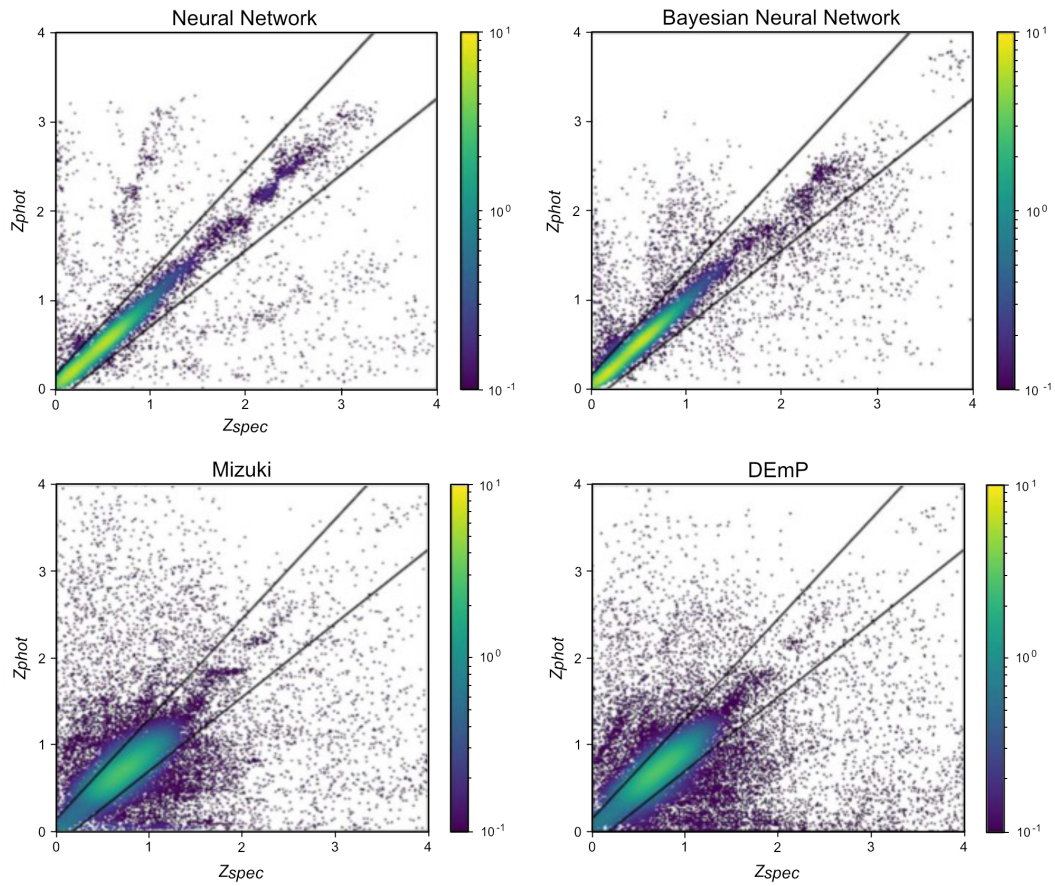


Figure 4: Visualization of predicted photo-zs vs. measured spectroscopic redshifts for a non-probabilistic neural network (top left), a Bayesian neural network (top right), and two previously proposed ML models (bottom left and right). Figure from [23]

References

- [1] Hiroaki Aihara et al. “First Data Release of the Hyper Suprime-Cam Subaru Strategic Program”. In: *Publications of the Astronomical Society of Japan* 70.SP1 (Jan. 2018). ISSN: 0004-6264, 2053-051X. DOI: 10.1093/pasj/psx081. (Visited on 06/18/2021).
- [2] Hiroaki Aihara et al. “Second Data Release of the Hyper Suprime-Cam Subaru Strategic Program”. In: *Publications of the Astronomical Society of Japan* 71.6 (Dec. 2019), p. 114. ISSN: 0004-6264, 2053-051X. DOI: 10.1093/pasj/psz103. arXiv: 1905.12221 [astro-ph]. (Visited on 08/16/2022).
- [3] Róbert Beck et al. “PS1-STRM: Neural Network Source Classification and Photometric Redshift Catalogue for PS1 3π DR1”. In: *Monthly Notices of the Royal Astronomical Society* 500.2 (Jan. 2021), pp. 1633–1644. ISSN: 0035-8711. DOI: 10.1093/mnras/staa2587. (Visited on 03/31/2024).
- [4] E. Bertin and S. Arnouts. “SExtractor: Software for Source Extraction.” In: *Astronomy and Astrophysics Supplement Series* 117 (June 1996), pp. 393–404. ISSN: 0365-01380004-6361. DOI: 10.1051/aas:1996164. (Visited on 01/17/2024).
- [5] M. Bilicki et al. “Photometric Redshifts for the Kilo-Degree Survey - Machine-learning Analysis with Artificial Neural Networks”. In: *Astronomy & Astrophysics* 616 (Aug. 2018), A69. ISSN: 0004-6361, 1432-0746. DOI: 10.1051/0004-6361/201731942. (Visited on 03/31/2024).
- [6] Christopher Bonnett. “Using Neural Networks to Estimate Redshift Distributions. An Application to CFHTLenS”. In: *Monthly Notices of the Royal Astronomical Society* 449.1 (May 2015), pp. 1043–1056. ISSN: 0035-8711. DOI: 10.1093/mnras/stv230. (Visited on 04/01/2024).
- [7] Bernadette M. Boscoe et al. “Elements of Effective Machine Learning Datasets in Astronomy”. In: *NeurIPS, Machine Learning for the Physical Sciences Workshop*. New Orleans, LA, Dec. 2022.
- [8] E. J. Bradshaw et al. “High-Velocity Outflows from Young Star-Forming Galaxies in the UKIDSS Ultra-Deep Survey”. In: *Monthly Notices of the Royal Astronomical Society* 433 (July 2013), pp. 194–208. ISSN: 0035-8711. DOI: 10.1093/mnras/stt715. (Visited on 08/16/2022).
- [9] S. Cavuoti et al. “Photometric Redshifts with the Quasi Newton Algorithm (MLPQNA) Results in the PHAT1 Contest”. In: *Astronomy & Astrophysics* 546 (Oct. 2012), A13. ISSN: 0004-6361, 1432-0746. DOI: 10.1051/0004-6361/201219755. (Visited on 04/01/2024).
- [10] Alison L. Coil et al. “The PRISM Multi-Object Survey (PRIMUS) I: Survey Overview and Characteristics”. In: *The Astrophysical Journal* 741.1 (Nov. 2011), p. 8. ISSN: 0004-637X, 1538-4357. DOI: 10.1088/0004-637X/741/1/8. arXiv: 1011.4307 [astro-ph]. (Visited on 08/16/2022).
- [11] Euclid Collaboration et al. *Euclid. I. Overview of the Euclid Mission*. May 2024. DOI: 10.48550/arXiv.2405.13491. arXiv: 2405.13491 [astro-ph]. (Visited on 06/06/2024).
- [12] Planck Collaboration et al. “Planck 2018 Results. VI. Cosmological Parameters”. In: *Astronomy & Astrophysics* 641 (Sept. 2020), A6. ISSN: 0004-6361, 1432-0746. DOI: 10.1051/0004-6361/201833910. arXiv: 1807.06209 [astro-ph]. (Visited on 08/24/2022).
- [13] Richard J. Cool et al. “The PRISM Multi-object Survey (PRIMUS). II. Data Reduction and Redshift Fitting”. In: *The Astrophysical Journal* 767.2 (Apr. 2013), p. 118. ISSN: 0004-637X, 1538-4357. DOI: 10.1088/0004-637X/767/2/118. arXiv: 1303.2672 [astro-ph]. (Visited on 08/16/2022).
- [14] A. D’Isanto and K. L. Polsterer. “Photometric Redshift Estimation via Deep Learning. Generalized and Pre-Classification-Less, Image Based, Fully Probabilistic Redshifts”. In: *Astronomy & Astrophysics, Volume 609, id.A111* 609 (Jan. 2018), A111. ISSN: 0004-6361. DOI: 10.1051/0004-6361/201731326. (Visited on 04/06/2022).
- [15] Marc Davis et al. “Science Objectives and Early Results of the DEEP2 Redshift Survey”. In: 4834 (Feb. 2003), pp. 161–172. DOI: 10.1117/12.457897. (Visited on 08/16/2022).
- [16] Sander Dieleman, Kyle W. Willett, and Joni Dambre. “Rotation-Invariant Convolutional Neural Networks for Galaxy Morphology Prediction”. In: *Monthly Notices of the Royal Astronomical Society* 450.2 (June 2015), pp. 1441–1459. ISSN: 0035-8711. DOI: 10.1093/mnras/stv632. (Visited on 07/22/2022).

- [17] M Eriksen et al. “The PAU Survey: Photometric Redshifts Using Transfer Learning from Simulations”. In: *Monthly Notices of the Royal Astronomical Society* 497.4 (Oct. 2020), pp. 4565–4579. ISSN: 0035-8711. DOI: 10.1093/mnras/staa2265. (Visited on 04/01/2024).
- [18] B. Garilli et al. “The VIMOS Public Extragalactic Survey (VIPERS): First Data Release of 57 204 Spectroscopic Measurements”. In: *Astronomy & Astrophysics* 562 (Feb. 2014), A23. ISSN: 0004-6361, 1432-0746. DOI: 10.1051/0004-6361/201322790. (Visited on 08/16/2022).
- [19] Ben Henghes et al. “Deep Learning Methods for Obtaining Photometric Redshift Estimations from Images”. In: *Monthly Notices of the Royal Astronomical Society* 512.2 (May 2022), pp. 1696–1709. ISSN: 0035-8711. DOI: 10.1093/mnras/stac480. (Visited on 04/02/2024).
- [20] Željko Ivezić et al. “LSST: From Science Drivers to Reference Design and Anticipated Data Products”. In: (May 2008). DOI: 10.3847/1538-4357/ab042c. (Visited on 08/16/2022).
- [21] Željko Ivezić et al., eds. *Statistics, Data Mining, and Machine Learning in Astronomy: A Practical Python Guide for the Analysis of Survey Data*. Princeton Series in Modern Observational Astronomy. Princeton, N.J: Princeton University Press, 2014. ISBN: 978-0-691-15168-7.
- [22] Evan Jones et al. “Improving Photometric Redshift Estimation for Cosmology with LSST Using Bayesian Neural Networks”. In: *The Astrophysical Journal* 964 (Apr. 2024), p. 130. ISSN: 0004-637X. DOI: 10.3847/1538-4357/ad2070. (Visited on 04/02/2024).
- [23] Evan Jones et al. *Photometric Redshifts for Cosmology: Improving Accuracy and Uncertainty Estimates Using Bayesian Neural Networks*. Feb. 2022. DOI: 10.48550/arXiv.2202.07121. arXiv: 2202.07121 [astro-ph]. (Visited on 08/16/2022).
- [24] O. Le Fèvre et al. “The VIMOS VLT Deep Survey Final Data Release: A Spectroscopic Sample of 35 016 Galaxies and AGN out to $z \sim 6.7$ Selected with $17.5 \leq i_{AB} \leq 24.75$ ”. In: *Astronomy & Astrophysics* 559 (Nov. 2013), A14. ISSN: 0004-6361, 1432-0746. DOI: 10.1051/0004-6361/201322179. (Visited on 08/16/2022).
- [25] Simon J. Lilly et al. “The zCOSMOS 10k-Bright Spectroscopic Sample”. In: *The Astrophysical Journal Supplement Series* 184 (Oct. 2009), pp. 218–229. ISSN: 0067-0049. DOI: 10.1088/0067-0049/184/2/218. (Visited on 08/16/2022).
- [26] Chris J. Lintott et al. “Galaxy Zoo: Morphologies Derived from Visual Inspection of Galaxies from the Sloan Digital Sky Survey”. In: *Monthly Notices of the Royal Astronomical Society* 389 (Sept. 2008), pp. 1179–1189. ISSN: 0035-8711. DOI: 10.1111/j.1365-2966.2008.13689.x. (Visited on 09/22/2022).
- [27] J. Liske et al. “Galaxy And Mass Assembly (GAMA): End of Survey Report and Data Release 2”. In: *Monthly Notices of the Royal Astronomical Society* 452 (Sept. 2015), pp. 2087–2126. ISSN: 0035-8711. DOI: 10.1093/mnras/stv1436. (Visited on 08/16/2022).
- [28] Rachel Mandelbaum. “Weak Lensing for Precision Cosmology”. In: *Annual Review of Astronomy and Astrophysics* 56.1 (2018), pp. 393–433. DOI: 10.1146/annurev-astro-081817-051928. (Visited on 09/29/2022).
- [29] R. J. McLure et al. “The Sizes, Masses and Specific Star-Formation Rates of Massive Galaxies at 1.3”. In: (May 2012). DOI: 10.1093/mnras/sts092. (Visited on 08/21/2022).
- [30] Ivelina G. Momcheva et al. “The 3D-HST Survey: Hubble Space Telescope WFC3/G141 Grism Spectra, Redshifts, and Emission Line Measurements for $\sim 100,000$ Galaxies”. In: *The Astrophysical Journal Supplement Series* 225.2 (Aug. 2016), p. 27. ISSN: 1538-4365. DOI: 10.3847/0067-0049/225/2/27. arXiv: 1510.02106 [astro-ph]. (Visited on 08/16/2022).
- [31] Yong-Huan Mu et al. “Photometric Redshift Estimation of Galaxies with Convolutional Neural Network”. In: *Research in Astronomy and Astrophysics* 20.6 (June 2020), p. 089. ISSN: 1674-4527. DOI: 10.1088/1674-4527/20/6/89. (Visited on 04/01/2024).
- [32] Jeffrey A. Newman and Daniel Gruen. “Photometric Redshifts for Next-Generation Surveys”. In: *Annual Review of Astronomy and Astrophysics* 60.1 (2022), pp. 363–414. DOI: 10.1146/annurev-astro-032122-014611. (Visited on 09/29/2022).
- [33] Jeffrey A. Newman et al. “The DEEP2 Galaxy Redshift Survey: Design, Observations, Data Reduction, and Redshifts”. In: *The Astrophysical Journal Supplement Series* 208.1 (Aug. 2013), p. 5. ISSN: 0067-0049, 1538-4365. DOI: 10.1088/0067-0049/208/1/5. arXiv: 1203.3192 [astro-ph]. (Visited on 08/16/2022).

- [34] Johanna Pasquet et al. “Photometric Redshifts from SDSS Images Using a Convolutional Neural Network”. In: *Astronomy & Astrophysics, Volume 621, id.A26*, <NUMPAGES>15</NUMPAGES> pp. 621 (Jan. 2019), A26. ISSN: 0004-6361. DOI: 10.1051/0004-6361/201833617. (Visited on 04/06/2022).
- [35] S. Schuldt et al. “Photometric Redshift Estimation with a Convolutional Neural Network: NetZ”. In: *Astronomy and Astrophysics* 651 (July 2021), A55. ISSN: 0004-6361. DOI: 10.1051/0004-6361/202039945. (Visited on 04/05/2022).
- [36] Christopher J. Shallue and Andrew Vanderburg. “Identifying Exoplanets with Deep Learning: A Five-planet Resonant Chain around Kepler-80 and an Eighth Planet around Kepler-90”. In: *The Astronomical Journal* 155 (Feb. 2018), p. 94. ISSN: 0004-6256. DOI: 10.3847/1538-3881/aa9e09. (Visited on 02/04/2021).
- [37] Rosalind E. Skelton et al. “3D-HST WFC3-selected Photometric Catalogs in the Five CANDELS/3D-HST Fields: Photometry, Photometric Redshifts, and Stellar Masses”. In: *The Astrophysical Journal Supplement Series* 214 (Oct. 2014), p. 24. ISSN: 0067-0049. DOI: 10.1088/0067-0049/214/2/24. (Visited on 08/16/2022).
- [38] Radamanthys Stivaktakis et al. “Convolutional Neural Networks for Spectroscopic Redshift Estimation on Euclid Data”. In: *IEEE Transactions on Big Data* 6.3 (Sept. 2020), pp. 460–476. ISSN: 2332-7790, 2372-2096. DOI: 10.1109/TBDATA.2019.2934475. (Visited on 04/01/2024).
- [39] Masayuki Tanaka et al. “Photometric Redshifts for Hyper Suprime-Cam Subaru Strategic Program Data Release 1”. In: *Publications of the Astronomical Society of Japan* 70.SP1 (Jan. 2018), S9. ISSN: 0004-6264. DOI: 10.1093/pasj/psx077. (Visited on 04/01/2024).
- [40] Ignacio Terrizzano et al. “Data Wrangling: The Challenging Journey from the Wild to the Lake”. In: ().
- [41] Angus H. Wright et al. “KiDS+VIKING-450: A New Combined Optical and near-Infrared Dataset for Cosmology and Astrophysics”. In: *Astronomy & Astrophysics* 632 (Dec. 2019), A34. ISSN: 0004-6361, 1432-0746. DOI: 10.1051/0004-6361/201834879. (Visited on 04/01/2024).

7 Appendix

In this Appendix, we present additional details for constructing the GalaxiesML dataset and show an example of its use.

8 HSC Database Queries

To obtain the initial list of galaxies for Step 1, we query the HSC PDR2 database to cross-match data from the HSC PDR2 imaging and photometry dataset with that of the spectroscopic dataset. Specifically, this query uses the `pdr2_wide.forced` and `pdr2_wide.specz` tables. The query also includes data quality filters as described in the main paper.

```
SELECT
  object_id
  , specz_redshift_err
  , specz_redshift
  , specz_mag_i
  , specz_name
  , specz_ra
  , specz_dec ,
specz_flag_homogeneous ,
  ra ,
  dec ,
  coord ,
  skymap_id ,
  g_cmodel_mag
  , r_cmodel_mag
  , i_cmodel_mag
  , z_cmodel_mag
  , y_cmodel_mag
```

```

        , g_cmodel_magsigma
        , r_cmodel_magsigma
          , i_cmodel_magsigma
            , z_cmodel_magsigma
              , y_cmodel_magsigma

FROM pdr2_wide.forced

LEFT JOIN pdr2_wide.forced2 USING (object_id)
LEFT JOIN pdr2_wide.specz USING (object_id)

WHERE
NOT
g_sdsscentroid_flag
  AND NOT
r_sdsscentroid_flag
  AND NOT
i_sdsscentroid_flag
  AND NOT
z_sdsscentroid_flag
  AND NOT
y_sdsscentroid_flag

AND NOT
  g_pixelflags_interpolatedcenter
AND NOT
  r_pixelflags_interpolatedcenter
AND NOT
  i_pixelflags_interpolatedcenter
AND NOT
  z_pixelflags_interpolatedcenter
AND NOT
  y_pixelflags_interpolatedcenter
AND NOT
  g_pixelflags_saturatedcenter
AND NOT
  r_pixelflags_saturatedcenter
AND NOT
  i_pixelflags_saturatedcenter
AND NOT
  z_pixelflags_saturatedcenter
AND NOT
  y_pixelflags_saturatedcenter
AND NOT
  g_cmodel_flag
AND NOT
  r_cmodel_flag
AND NOT
  i_cmodel_flag
AND NOT
  z_cmodel_flag
AND NOT
  y_cmodel_flag
AND NOT
  g_pixelflags_edge
AND NOT
  r_pixelflags_edge

```

```

AND NOT
i_pixelflags_edge
AND NOT
z_pixelflags_edge
AND NOT
y_pixelflags_edge
AND NOT
g_pixelflags_crcenter
AND NOT
r_pixelflags_crcenter
AND NOT
i_pixelflags_crcenter
AND NOT
z_pixelflags_crcenter
AND NOT
y_pixelflags_crcenter
AND NOT
g_pixelflags_bad
AND NOT
r_pixelflags_bad
AND NOT
i_pixelflags_bad
AND NOT
z_pixelflags_bad
AND NOT
y_pixelflags_bad
AND specz_redshift > 0
AND 0 < specz_redshift_err
AND specz_redshift_err < 1
AND specz_redshift < 9.999

```

9 HSC Image Query

Images were obtained by uploading the ra and dec positions in batches of 100,00 requests at a time to the HSC Image Cutout Service at: https://hsc-release.mtk.nao.ac.jp/das_cutout/pdr2/manual.html#list-to-upload. Here is a example of some of the lines from the positional query:

#?	rerun	filter	ra	dec	sw	sh		
	pdr2_wide	HSC-Y	31.73471487	-6.610750394	10 arcseconds	10 arcseconds		
	pdr2_wide	HSC-Y	31.19229445	-6.44807734	10 arcseconds	10 arcseconds		
	pdr2_wide	HSC-Y	31.20098659	-6.878016245	10 arcseconds	10 arcseconds		
	pdr2_wide	HSC-Y	31.09620369	-6.250176133	10 arcseconds	10 arcseconds		
	pdr2_wide	HSC-Y	31.16933934	-6.523789799	10 arcseconds	10 arcseconds		

10 Source Extractor Configuration

We use the software Source Extractor [4] to measure the shape and flux distribution of the galaxies in the GalaxiesML dataset. The fit parameters are described in the main text. Source Extract requires both a parameter file and a configuration file to run. Here we give examples of these files.

We use the following parameter file running Source Extractor on each image:

```

NUMBER      1                #Running object number
DETECT_THRESH 3
CATALOG_NAME output_image
CATALOG_TYPE ASCII_HEAD
CHECKIMAGE_TYPE SEGMENTATION
PETRO_RADIUS 1
PETRO_TYPE AUTO
X_IMAGE 60
Y_IMAGE 60
XMIN_IMAGE 57.5

```

```

XMAX_IMAGE 62.5
YMIN_IMAGE 57.5
YMAX_IMAGE 62.5
ISOAREA_IMAGE 0.0
ISOAREA_WORLD 0.0
A 0.0
B 0.0
A_IMAGE
B_IMAGE
THETA_IMAGE 0.0
THETA_WORLD 0.0
MU_MAX 0.0
ELLIPTICITY 0.0
SERSIC 0.0
PHOT_TYPE SERSIC
PHOT_AUTOPARAMS 2.5, 3.5
PHOT_APERTURES 5
FLUX_RADIUS
SPHEROID_SERSICN 4.0
SPHEROID_RE 10.0

```

We use the following configuration file running Source Extractor on each image:

```

# Default configuration file for SExtractor 2.25.0
# EB 2021-05-31
NUMBER 1
PETRO_TYPE AUTO
PETRO_THRESH 0.2
#----- Catalog -----
CATALOG_NAME test.cat # name of the output catalog
CATALOG_TYPE ASCII_HEAD # NONE, ASCII, ASCII_HEAD, ASCII_SKYCAT,
# ASCII_VOTABLE, FITS_1.0 or FITS_LDAC
PARAMETERS_NAME default.param # name of the file containing catalog contents
#----- Extraction -----
DETECT_TYPE CCD # CCD (linear) or PHOTO (with gamma correction)
DETECT_MINAREA 5 # min. # of pixels above threshold
DETECT_THRESH 1.5 # <sigmas> or <threshold>,<ZP> in mag.arcsec-2
ANALYSIS_THRESH 1.5 # <sigmas> or <threshold>,<ZP> in mag.arcsec-2
FILTER Y # apply filter for detection (Y or N)?
FILTER_NAME gauss_1.5_3x3.conv # name of the file containing the filter
DEBLEND_NTHRESH 32 # Number of deblending sub-thresholds
DEBLEND_MINCONT 0.005 # Minimum contrast parameter for deblending
CLEAN Y # Clean spurious detections? (Y or N)?
CLEAN_PARAM 1.0 # Cleaning efficiency
MASK_TYPE CORRECT # type of detection MASKing: can be one of
# NONE, BLANK or CORRECT
#----- Photometry -----
PHOT_APERTURES 5 # MAG_APER aperture diameter(s) in pixels
PHOT_AUTOPARAMS 2.5, 3.5 # MAG_AUTO parameters: <Kron_fact>,<min_radius>
PHOT_PETROPARAMS 2.0, 3.5 # MAG_PETRO parameters: <Petrosian_fact>,
# <min_radius>
SATUR_LEVEL 50000.0 # level (in ADUs) at which arises saturation
SATUR_KEY SATURATE # keyword for saturation level (in ADUs)
MAG_ZEROPOINT 0.0 # magnitude zero-point

```

```

MAG_GAMMA      4.0          # gamma of emulsion (for photographic scans)
GAIN            0.0          # detector gain in e-/ADU
GAIN_KEY       GAIN         # keyword for detector gain in e-/ADU
PIXEL_SCALE    0.17        # size of pixel in arcsec (0=use FITS WCS info)

PHOT_TYPE      SERSIC
SERSIC_FIT     Y
FIT_PROFILE     N
#----- Star/Galaxy Separation -----

SEEING_FWHM    1.2          # stellar FWHM in arcsec
STARNNW_NAME   default.nnw # Neural-Network_Weight table filename

#----- Background -----

BACK_SIZE      64           # Background mesh: <size> or <width>,<height>
BACK_FILTERSIZE 3           # Background filter: <size> or <width>,<height>

BACKPHOTO_TYPE GLOBAL      # can be GLOBAL or LOCAL

#----- Check Image -----

#CHECKIMAGE_TYPE -BACKGROUND # can be NONE, BACKGROUND, BACKGROUND_RMS,
# MINIBACKGROUND, MINIBACK_RMS, -BACKGROUND,
# FILTERED, OBJECTS, -OBJECTS, SEGMENTATION,
# or APERTURES
#CHECKIMAGE_NAME check.fits # Filename for the check-image

#----- Memory (change with caution!) -----

MEMORY_OBJSTACK 3000       # number of objects in stack
MEMORY_PIXSTACK 300000    # number of pixels in stack
MEMORY_BUFSIZE  1024      # number of lines in buffer

#----- Miscellaneous -----

VERBOSE_TYPE    NORMAL     # can be QUIET, NORMAL or FULL
HEADER_SUFFIX   .head      # Filename extension for additional headers
WRITE_XML       N          # Write XML file (Y/N)?
XML_NAME        sex.xml    # Filename for XML output
DETECT_THRESH  3           #Running object number
NUMBER          1
DETECT_THRESH  3
CATALOG_NAME    output_image
CATALOG_TYPE    ASCII_HEAD
CHECKIMAGE_TYPE SEGMENTATION
ERRXY_IMAGE     5

```

11 Redshift estimation using convolutional neural network with images and photometry

We demonstrate the improvements that can be made by including imaging information by developing a hybrid convolutional neural network (CNN) that includes both images and photometry. We use a CNN architecture with 7 convolutional layers (with 3×4 kernels) and 5 pooling layers, inter-dispersed between the convolutional layers. A novel aspect of our network is the inclusion of photometry as well, which has inputs for the five-band photometry and 6 dense layers. The photometric network is connected to the output of the CNN, which then goes through three additional fully connected layers.

We train the data using the 127×127 pixel size images and g, r, i, z, y magnitudes as the inputs and the spectroscopic redshift as the label. We use 204,573 galaxies for training, 40,914 galaxies for validation, and 40,914 galaxies for testing. The validation set is used for hyperparameter optimization while the testing data set is used for final performance evaluation since that dataset has been isolated

Model	N galaxies	Loss	Bias	Scatter	Outlier Fraction	MSE
CNN	40914	0.0577	0.000100	0.0167	0.0377	0.0615
NN	40914	0.106	0.00110	0.0315	0.0688	0.133

Table 2: Overall performance metrics for NN and CNN models

from the model. We trained the model for 200 epochs and utilized a batch size of 256. During training, we utilize the custom loss function from [39]:

$$L = 1 - \frac{1}{1 + \left(\frac{z_{phot} - z_{spec}}{0.15(1+z_{phot})}\right)^2}, \quad (1)$$

where z_{phot} is the photometric redshift prediction and z_{spec} is the spectroscopic redshift.

We also use the Adam optimization algorithm with a learning rate of 0.0001 ([kingma2014]). The training was performed on a desktop computer using an AMD Ryzen Threadripper PRO 3955WX with 16-Cores and NVIDIA RTX A6000 GPU with 48 GB of GPU RAM. The training used the 127×127 pixel dataset and 5-band photometry typically took 48-96 hours and used 20 GB of GPU memory.

To evaluate the performance of the two types of neural networks, we use common metrics for photometric redshift estimates: bias, scatter, RMS error, and outlier rate. The bias, b , is defined as:

$$b = \frac{z_{phot} - z_{spec}}{1 + z_{spec}}. \quad (2)$$

The RMS error is:

$$rms = \sqrt{\frac{1}{n_{gals}} \Sigma_{gals} \left(\frac{z_{phot} - z_{spec}}{1 + z_{spec}}\right)^2}, \quad (3)$$

where n_{gals} is the number of galaxies. The scatter or dispersion is defined with respect to the median absolute error (MAD):

$$\sigma_{scatter} = 1.48 \times \text{Median}(|\Delta z_i - \text{Median}(\Delta z_i)|), \quad (4)$$

where $\Delta z_i = z_{phot,i} - z_{spec,i}$ for the i th galaxy. Note the scale factor of 1.48 is to make the MAD more comparable to the standard deviation of a normal distribution. The outlier, O , is defined as:

$$O = \frac{|z_{phot} - z_{spec}|}{1 + z_{spec}} > .15. \quad (5)$$

The outlier fraction is defined as the fraction of outliers divided by the total number of galaxies:

$$f_{outlier} = N_{outliers}/N_{total}. \quad (6)$$

We also use the mean-squared error and the loss as additional metrics. We evaluate these performance metrics in different redshift bins to study the model performance at different redshifts. The number of galaxies in the training set varies significantly between different redshift bins so it is important to assess potential biases with redshift.

We find that the CNN models using images show better predictive performance than the NN models using only photometry (Table 2). The biggest improvement is the bias where the CNN outperforms the NN by about a factor of 10 on average (NN $b = 0.0011$, CNN $b = 0.00010$). In addition, the improvement in the model performance with the CNN compared to the NN is larger at higher redshifts. This gap in performance is especially large at the $z = 1.5$, the highest redshift we consider in this example. The number of galaxies in the training set at this redshift bin is significantly smaller than at other redshift bins. This likely indicates that the images can encode more information about the redshift than photometry alone, which allows the CNN to achieve higher performance with a smaller training sample compared to the NN with photometry.

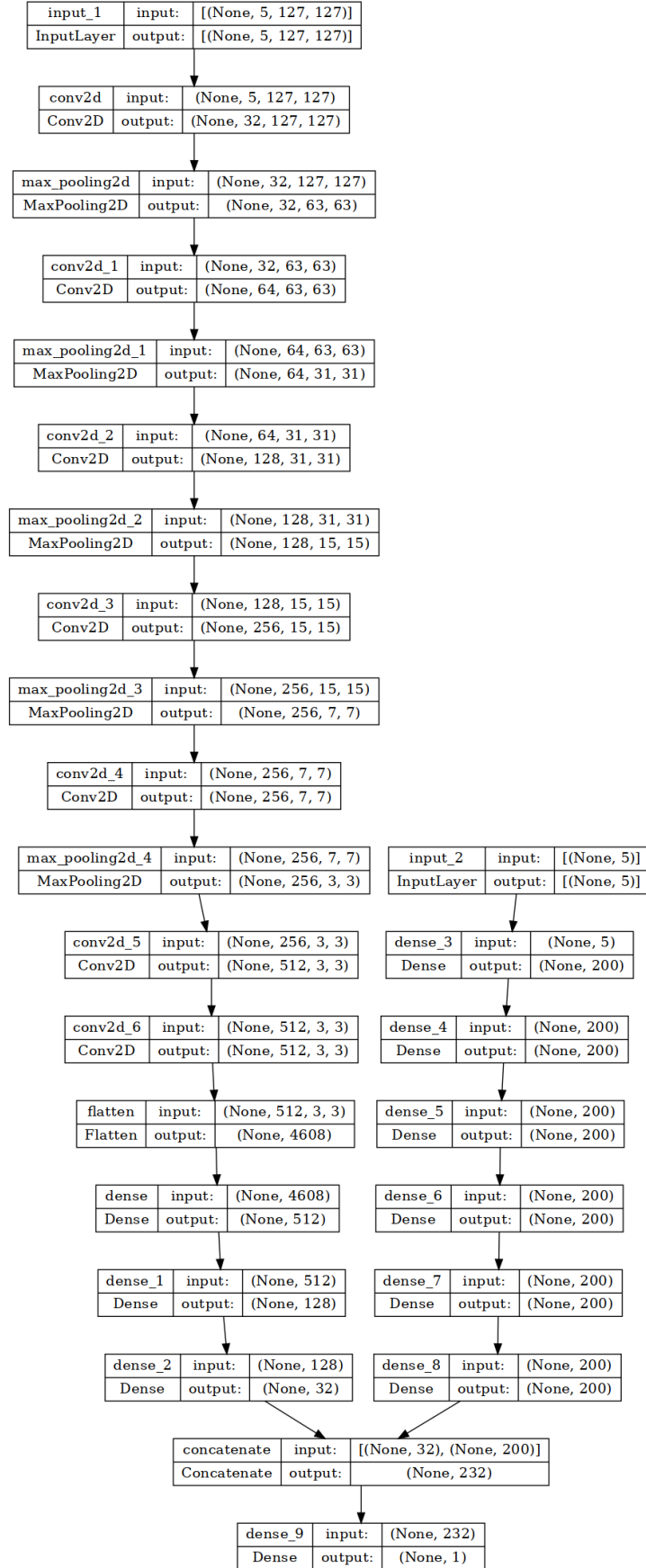


Figure 5: CNN architecture for this work. The model includes both images and photometry.

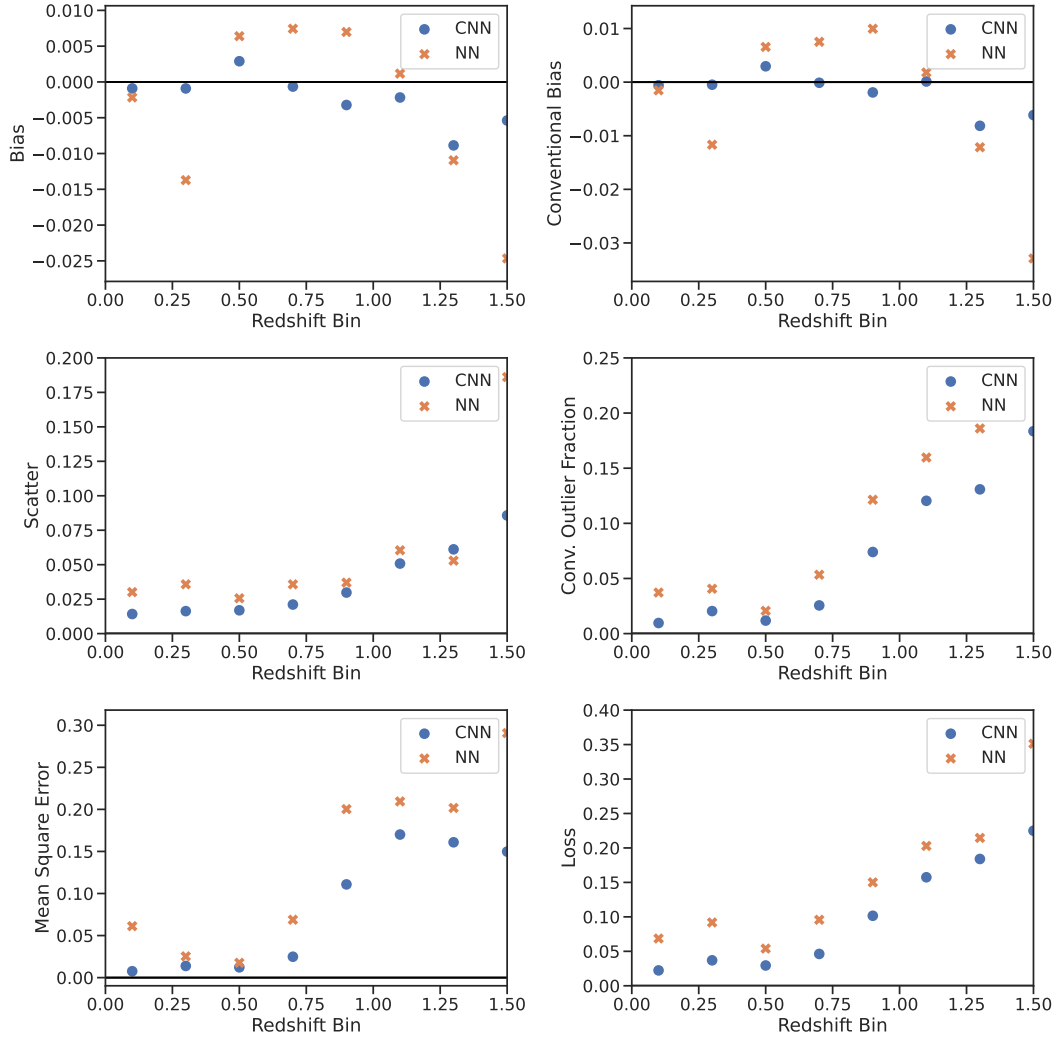


Figure 6: Metrics for the performance of the NN compared to the CNN at different redshift ranges for (a) bias, (b) scatter, (c) outlier fraction, (d) MSE, and (e) loss. The smaller the values are for these metrics, the better the model. The CNN model using images outperforms the NN model using only photometry, especially at larger redshifts where there is less training data.